Crustal structure and contact relationship revealed from deep seismic sounding data in South China

Zhongjie Zhang, Yanghua Wang

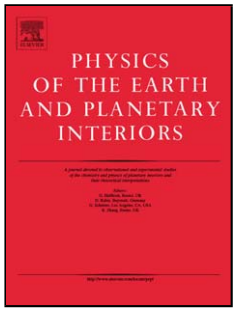

Title: Crustal structure and contact relationship revealed from deep seismic sounding data in South China

Authors: Zhongjie Zhang, Yanghua Wang

PII: S0031-9201(07)00190-2
DOI: doi:10.1016/j.pepi.2007.08.005
Reference: PEPI 4865

To appear in: *Physics of the Earth and Planetary Interiors*

Received date: 3-12-2006
Revised date: 3-8-2007
Accepted date: 31-8-2007

Please cite this article as: Zhang, Z., Wang, Y., Crustal structure and contact relationship revealed from deep seismic sounding data in South China, *Physics of the Earth and Planetary Interiors* (2007), doi:10.1016/j.pepi.2007.08.005

Crustal structure and contact relationship revealed from deep seismic sounding data in South China

Zhongjie Zhang[a] and Yanghua Wang[b]

[a] Chinese Academy of Sciences, State Key Laboratory of Lithosphere Evolution, Institute of Geology and Geophysics, Beijing 100029, China
[b] Imperial College London, Centre for Reservoir Geophysics, Department of Earth Science and Engineering, London SW7 2AZ, UK

Abstract

A 400 km-long wide-angle seismic profile in the South China crosses three tectonic domains: southeast continental margin of Yangtze block, northwest continental margin of Cathaysia block, and South China Suture Zone separating these two blocks. The crustal velocity model constructed from traveltime fitting shows that the crust thickness thins from the northwest to the southeast along the profile. It also reveals the crustal contact relationship between the Yangtze and Cathaysia blocks, where the Wuchuan-Sihui fault is the boundary between them. Combining this profile with two more profiles in the continental South China and three profiles in the northern margin of South China Sea, constructs a continent-ocean transition section. This cross-section reveals that the Moho depth shallows gradually along the cross-section from the Yangtze block to the Cathaysia block and the northern margin of South China Sea, but shallows abruptly in the continent-ocean transition to the South China Sea.

Keywords: crustal structure, wide-angle seismic data, continent-ocean transition, Yangtze block, Cathyasia block, South China

1. Introduction

The South China tectonic regime (Figure 1) refers to a segment within the eastern margin of Eurasia. It is characterized by a complicated structural pattern (Zhang *et al.*, 1984;

Angelier, 1990; Hou and Li, 1993), and consisted of three main elements: the southeast continental margin of Yangtze block, the northwest continental margin of Cathaysia, and the boundary of South China suture zone (SCSZ) between Yangtze and Cathaysia blocks. The main purpose of this paper is to study the crustal velocity structure of the Yangtze and Cathaysia blocks and crustal contact relationship between these two blocks.

The South China continent, located at the continental margin of western Pacific Ocean, endured the subduction of western Pacific Plate. Since Grabau (1924) first used Cathaysia to describe the geology of southeast China and part of the coastal region of West Pacific, it has been about 80 years dispute on regional tectonics, and much of the disputation has been focused on whether or not 'Cathaysia' really exists, its distribution and tectonic evolution (Huang, 1980; Guo *et al.*, 1983; Yang *et al.*, 1986; Yin and Nie, 1993; Zhang *et al.*, 1994). Several authors suggested that such an old continental mass is present (Shui, 1988; Jahn *et al.*, 1990; Wang and Liu, 1992) but its distribution remains controversial (Shui, 1988; Ren *et al.*, 1990).

In the recent 20 years, several tectonic models have been postulated to account for the Mesozoic tectonic evolution of the South China block (Jahn *et al.*, 1986, 1990; Rodgers, 1989; Rowley *et al.*, 1989; Hsü *et al.*, 1990; Charvet *et al.,* 1996; Liu *et al.*, 1996; Li *et al.*, 2000; Zhou and Li, 2000; Wang *et al.*, 2003). These models include Andean-type active continental margin (Guo *et al.*, 1983), Alps-type collision belt (Hsü *et al.*, 1988, 1990), and lithospheric subduction (Holloway, 1982; Faure, 1996; Zhou and Li, 2000) with underplating of mafic magma. These models suggest that the tectonic regime was dominantly compressive as the result of either westward subduction of a Mesozoic Pacific plate, or the closure of an oceanic basin in the South China block interior (Holloway, 1982; Hsü *et al.*, 1990; Faure, 1996; Zhou and Li, 2000). Alternative models include wrench faulting (Xu *et al.,* 1993) and continental rifting and extension (Gilder *et al.*, 1996; Li *et al.*, 2000; Wang *et al.*, 2003). These models suggest that intracontinental lithospheric extension and thinning dominated since the early Mesozoic (Li *et al.*, 1989; Faure, 1996; Gilder *et al.*, 1996; Li *et al.*, 2000; Wang *et al.*, 2003).

In order to study its structures, its composition and the evolution of the lithosphere in the South China and its adjacent sea, Chinese Academy of Sciences (CAS) carried out

various research projects involving multi-disciplinary integrated studies including geodynamics, marine geology, geochemistry and geophysics experiments between mid-1980s and 1990s (Wei *et al.*, 1990; Li, 1992; Zhang *et al.*, 2000). Among these projects, the CAS Institute of Geophysics in 1990 conducted a deep seismic sounding experiment between Lianxian and Gangkou Island (Figure 1). In the present paper, we report our interpretation result of this 400 km-long deep seismic sounding profile. We describe the crustal structure model, its velocity distribution and major crustal penetrating faults along the profile, in particular the crustal boundary between the Yangtze and Cathaysia blocks. We also combine this profile with other two profiles in the South China continent and three profiles in the northern margin of South China Sea (Nissen *et al.*, 1995a, b; Yan *et al.*, 2001), to construct a cross-section across the Yangtze block, the Cathaysia block, the north margin of South China Sea, and the South China Sea. This cross-section clearly reveals the lateral variation across the continental margin of South China Sea.

1.1 Tectonic background

Within the tectonic unit of South China, the Yangtze block and the Cathaysia block were consolidated along the so-called South China Suture Zone (SCSZ) at ca. 970 Ma (Li and McCulloch, 1996). The basement rocks of the Yangtze block have an average age of 2.7-2.8 Ga (Qiu *et al.,* 2000) with the oldest of >3.2 Ga. In contrast, basement of the Cathaysia block exhibits Paleo- to Mesoproterozoic and possibly late Archean ages of about 2.5 Ga (Chen and Jahn, 1998; Wang *et al.*, 2003).

The South China continental is featured with distinctive aged sedimentary and igneous rocks. As shown in Figure 1, late Mesozoic magmatic rocks, consisting predominantly of granite and rhyolite with an outcrop area of 95%, are spread across a 600 km belt along the coastline of southeastern China (Wang *et al.*, 2003). Across the continental, volcanic rocks occur mainly in the eastern part of South China Suture Zone (SCSZ in Figure 1), and the western board of this volcanic belt is located at about 450 km away from this belt. Igneous rocks in South China fall into three main age groups, early Yanshanian (180-160 Ma), mid Yanshanian (160-140) and late Yanshanian (140-97 Ma)

(Wang *et al.*, 2003). In some areas, the late Yanshanian group includes rocks as young as ca.79 Ma (Martin *et al.*, 1994). The early Yanshanian volcanism belongs to a K-rich calc-alkaline series inter-layered with continental or shallow water detrital rocks (Wu and Qi, 1985; Zheng, 1985; Zhang, 1989). Conversely, the late Yanshanian volcanism, of bimodal character, is associated with continental red beds along NE-SW-trending grabens, indicative of intracontinental rifting. Granitoids present a wide variety of petrographic types from biotite-granite to tonalite. Peraluminous granitoids formed by crustal melting are also common (Tu *et al.*, 1980; Jahn *et al.*, 1990). The proportion of volcanic rock increase oceanward (Zeng *et al.*, 1997; Zhou and Li, 2000; Wang *et al.,* 2003).

2. The wide-angle seismic profile

The wide-angle deep seismic sounding experiment profile (Figure 1) crosses the southern continental margin of Yangtze block, the southeastern continental margin of Cathaysia block, and the South China suture zone between these two blocks with different aged basement, and provides a good opportunity to reveal their crustal structures. The 400-km-long seismic profile with azimuth nearly N30W runs from Lianxian, near Hunan Province, to Gangkou Island, near Guangzhou City. Along the profile, there are a series of NE faults (Wuchuan-Sihui faults: F_1; Enping-Xinfeng: F_2; Heyuan-Zengcheng: F_3; Zijjin-Boluo: F_4; and Lianhuashan: F_5) (Huang, 1980; Wang *et al.*, 2003).

In this experiment, shots were fired at six sites, Lianxian (LX), Dawan (DW), Qingyuan (QY), Conghua (CH), Boluo (BL) and Gangkou Island (GK), and three-component DZSS-1 seismographs were deployed along the profile through. The shot at Gangkou was detonated in the waters of the coastal South China Sea. The remaining five shots consisted of a pattern of holes drilled to a depth of 20 m and loaded with a charge ranging from 1,500 to 2,000 kg of explosive. A total of 100 portable three-component seismic stations were installed along the survey profile. All the stations and shots were located using 1:25,000 topographic maps with an estimated location accuracy of 12.5 m. The seismic signals recorded by the seismographs were initially sampled at a rate of 2.5 ms, and then filtered within the 1-8 Hz frequency band for P-waves. Figure 2 displays shot gathers at a reduced

time scale using for a velocity of 6.0 km/s.

The upper panels of Figures 2a-f show the six shot gathers with the interpretation of *P*-wave events. Except the shot gather at LX (Figure 2a), all other seismograms exhibit a high signal-to-noise ratio for *Pg* arrivals refracted above of the crystalline basement and *Pm*-waves (*Pm* is equivalent to *PmP*, Moho reflection) with strongest amplitudes reflected from the Moho. The *Pn*-waves (Moho head/festooning wave), refracted from the Moho, are identified even though their amplitudes are weak compared with the amplitude of the Moho reflection phases. The lower panels of Figures 2 a-f display the modelled raypaths corresponding to these reflections.

The maximum visible recorded offset for event *Pg* is 40-60 km on all shot gathers, 20-40 km shorter than recorded in other places in the South China (Zhang *et al.*, 2005). This may indicate the lateral (compositional) heterogeneity of sedimentary cover in the South China. Generally, the *Pg* traveltime is about 0.5 s for the shots located near to west of shot CH. The *Pg* traveltime of southeast branch of shot CH gather is delayed, compared to its northwest branch, and such delay is also evidenced in shot gathers at BL and GK. This *Pg* traveltime change along the profile clearly demonstrates the abrupt change of the *P*-wave velocity above the crystalline basement. Part of this velocity variation is due to the presence of the sediments in the sedimentary basin (Huiyuan basin, Figure 3) and asymmetry in the Quaternary sediments of Minzhong and Lianshan Depressions (Figure 3) to the northwest of CH.

Four *P*-wave events P1-P4, reflected from interfaces within crust, are identified. In some portions of the data the reverbatory nature of the arrivals makes it hard to distinguish the onsets of each specific phase (e.g. CH shot to the northwest, ranges 50 to 100 km, at 1-3 s, Figure 2d). When interpreting sparse data such as these where signal-to-noise ratio is low, although the seismic responses from the Moho and the upper mantle are so strong, it can be hard to convincingly prove that one phase correlation is better than another (e.g., for shot QY to the northwest offsets > 60 km). To satisfactorily explain the observed seismic energy on the clearest data requires at least four separate intra-crustal phases (e.g. for shot GK to the northwest, Figure 2f). These intra-crustal reflections (labeled *P1-P4*) could be originating from the topography undulation of the topmost of mantle, discontinuous

reflectors or intra-crustal self-organization structure (Poppeliers and Levander, 2004). As we assume the lower-crustal reflector in our model to be laterally continuous, we show the calculated phases even where the arrivals are barely visible from the data. For example, regarding to the *P3* reflection in shot CH to the northwest, where the data are locally weak and noise, our model is not well-constrained by the data in this particular instance.

The amplitudes of reflection events *P1* (upper crust), *P2* and *P3* (middle crust) and *P4* (lower crust) are relatively weak compared with the event *Pm*. This is a general feature also observed in other wide-angle seismic experiments in the South China (Yuan *et al.*, 1989; Wei *et al.*, 1990; Zhang *et al.*, 2005). The event *Pm* is traceable from 80 to 160 km. The refracted event *Pn*, although weak, is sufficiently clear to be identified. The analysis of these phases reveals a *P*-wave velocity about 8.0-8.1 km/s in the uppermost of mantle. For many of the late-arriving phases there are large uncertainties in picking the arrival times (as much as 0.2 s) corresponding to uncertainties in the crustal structure of the order of 1-2 km, or equivalently the variations of P-wave velocities. These uncertainties may reduce, but probably cannot completely eliminate, the inferred lateral variation in crustal thickness from northwest to southeast. For the above-mentioned reasons, we admit that the interpretation of this wide-angle seismic experiment can only reveal a first-order variation in crustal properties along the profile.

3. Crustal structure along the seismic profile

Figures 3a and 3b show the *P*-wave velocity model of the upper part and the whole of the crust, obtained for the Lianxiang-Gangkuo wide-angle seismic profile. For constructing this crustal velocity model, we have implemented an interpretation by fitting the field observations with theoretical traveltimes from the ray tracing (Červený *et al.,* 1977). In our traveltime fitting, the residual (the difference between observed and calculated traveltimes) for the events P1 to Pm is less than 0.025 s per observed station. But the uncertainties are mostly coming from the picking of observed traveltimes. For many of the late-arriving phases, there are as large as 0.2 s uncertainties in picking the arrival times, corresponding

to the uncertainties in the crustal structure as order of about 1.3 km $(\approx \pm 0.2\,\mathrm{s} \times 6.3\,\mathrm{km/s})$.

The crust-uppermost mantle model we proposed here consists of a series of semi-horizontal layers in which *P*-wave velocity changes both vertically and horizontally, and is similar to those proposed for other parts of the South China block (Yuan *et al.*, 1989; Wei *et al.,* 1990; Zeng *et al.*, 1997; Zhang *et al.*, 2000, 2005). On the basis of traveltime fitting, we can summarize the crustal structure along the Lianxian-Gangkou profile from our crustal P-wave velocity model: (1) The average thickness of the crust is about 34 km beneath the Yangtze block, thinning gradually from northwest to southeast. (2) The average *P*-wave velocity for the crust is about 6.3 km/s. (3) The apparent *P*-wave velocity of the event P3 is slower than that of the event P2. The latter suggests that there is possibility of one lower velocity layer between reflector P2 and P3, even though constrains about the existence of lower velocity layer are not powerful with the field experiment limitation. In our final model, there is a relatively narrow lower velocity layer with thickness of about 5 km and *P*-wave velocity of 5.8 km/s.

3.1 Upper crust velocity structure

The upper crust consists of the sedimentary cover and one underlie layer. The sedimentary cover extends over this structure along the profile with variable thickness of about 4 km at the northwest of the Wuchuan-Sihui fault, 6-7 km under Minzhong Depression (between Qinyuan and Conghua) and Huiyuan Basin (Between Qinyuan and Gangkuo), thinner than 4 km between Lianshan Depression and Huiyuan Basin (Figure 3). The *P*-wave velocity of sedimentary varies considerably across the basin with velocity typically <5.8 km/s at the northwest side of Wuchuan-Sihui fault and velocity of >5.8 km/s typically in the area southeast side of this fault. Good correlation exists between the computed velocity model and the mapped geological formations (GBGMR, 1989). In particular, the regions of relatively high velocity coincide with zones where Carboniferous limestone and dolomite crop out near the surface (V_p = 5.8 km/s, 0-100 km along the profile, Figure 3a), and low-velocity zones are associated with the presence of Quaternary sediments and Late Jurassic granite (V_p = 4.5 km/s, 150-200 km, Minzhong Depression in

Figures 3a and 3b) or early granite (V_p = 5.0 km/s, 240-280 km), sedimentary basins or volcanic material (V_p = 5.1 km/s; 300-400 km, Huiyuan Basin in Figures 3a and b). The large-scale faults (F_1, F_2, F_3 and F_4 in Figure 1) are closely related to the abruptly lateral variations of the seismic velocity shown in Figure 3a.

There is one layer with P-wave velocity between 6.0 and 6.15 km/s underlie the sedimentary cover. The layer thickness under the Yangtze block (about 6-7 km) is 2-3 km thicker than that of the Cathaysia block. The bottom of the upper crust (which produces the P1 reflection) at a depth of about 10 km, undulates remarkably along the whole profile (Figure 3a and Figure 3b). Beneath the Cathaysia (southeastward from about 120 km along the profile), there is a strong lateral heterogeneity of *P*-wave velocities. The marked change in depth at about 100 km along the profile corresponds to the depth that Wuchuan-Sihui fault (F_1 in Fig.1) penetrates. Many features along the profile, there are abrupt variations that correspond to depth penetrated by the faults Enping-Xinfeng (160-180 km, F_2 in Figure1), Heyuan-Zengcheng fault (about 240 km, F_3), Zhijin-Boluo fault (about 280 km, F_4) and Lianhuashan fault (360 km, F_5).

3.2 Middle and lower crust velocity structure

The middle crust thins from 8 km thick (depth range between 10 and 18 km) at Lianxian in the northwest, to 11 km (depth range of 8-19 km) at Gangkou in the southeast.

The middle crust contains two layers that give rise to the branches P2 and P3 marked on the record sections (Figure 2, upper panels). There are no convincing crossovers between P2 and P3 similar to other wide-angle seismic profiles acquired in the South China block (Yuan *et al.*, 1989; Zhang *et al.*, 2005), and events P2 and P3 have almost the same apparent *P*-wave velocity. These may imply that there is a low velocity gradient zone or lower velocity layer, and that the P2 and P3 events are the reflections from the top and the bottom of a low-velocity layer at the base of the middle crust. In Figure 3b, this thin low-velocity layer with 5 km thickness, sandwiched between the reflectors P2 and P3, shows P-wave velocity value of 5.8 km/s, whereas the upper layer is characterized with *P*-wave velocity of 6.2-6.3 km/s. However, this low-velocity layer is not convincingly

established with this wide-angle seismic experiment.

We analyze two explanations for the lower velocity layer at the bottom of middle crust. The first one is that this low velocity zone represents a ductile shear zone (Zhou and Li, 2000). The support evidences of this first explanation include: (a) The Q_p-value of the layer is low, about 40-100 obtained with seismic amplitude spectral ratio method from the wide-angle seismic interpretation between Hengyang and Quanzhou profile (Yuan *et al.*, 1989); (b) The occurrence of hot springs at the surface may derived from these ductile shear zone or high heat conductivity body (Yuan *et al.*, 1989). The second explanation is that the low-velocity layer has been strongly altered by the presence of partially molten rock.

The lower crust is about 13 km thick and is divided of two layers each with a very irregular contact that give rise to the branches *P4* and *Pm* marked as seismic reflections on the record sections. The *P*-wave velocity increases quickly to 6.5-6.6 km/s for the materials immediately below the middle crust and then takes values of 6.7-6.8 km/s in the upper half of the lower crust. The lower crust exhibits no strong lateral variations in velocity. Note that we cannot exclude the lateral heterogeneity of seismic velocity in the lower crust, as our wide-angle seismic experiment cannot reconstruct small-scale *P*-wave velocity heterogeneities in the lower crust.

3.3 Moho discontinuity

The crust gradually thins from northwest to southeast. The maximum depth of the crust is 34 km at Lianxian and about 32 km at Gangkou (Figure 3b). The Moho topography along the Lianxian-Gangkou profile is predominantly featured with its geometrical rise beneath the middle segment (120-260 km) of the profile. The thinner crust in the centre of the model interrupts the general seaward thinning, which can be demonstrated by the locally significant gravity effect shown in the upper panel Figure 3c. These results are consistent with *Pm* traveltimes variations of 0.5 s delay between the shot GK and the shot DW. This interpretation is consistent with the Moho depth variation along other profiles in the South China, such as it's about 36 km under Tunxi (Figure 5, to the northwest of the

South China) and about 30 km at Dongtou (to the southeast) along the Tunxi-Wenzhou profile (Zhang *et al.*, 2005), it's about 38 km under Hengyang (Figure 5, to the northwest of the South China) and 30 km at Quanzhou along the Hengyang-Quanzhou profile (Yuan *et al.*, 1989).

The reflection amplitudes observed from the crust-mantle boundary are sufficiently strong to suggest that there is no significant partial melt in the lower crust. There are multiple refracted *Pn*-phases recorded after the *Pm* arrivals for shots DW and CH (Pn, Pn1 and/or Pn2, in Figures 2b and 2d). The variability and complexity of the Pn events could be due to mantle topography that produces the irregular scattering from the Moho interface (Zhang *et al.*, 2000) or stochastic structure underlying Moho (Poppeliers and Levander, 2004). Therefore, there should be a complicate topography presented in the crust-mantle boundary, if there is an abrupt velocity discontinuity, and otherwise a transition zone enhanced by a strong velocity gradient (Zhang *et al.*, 2000; Lin and Wang, 2005).

3.4 Velocity variation versus gravity variation

Considering the shot-recorder arrangements and ray trajectories from different reflectors including the Moho, we infer that the different layers are sufficiently imaged. Most portions of the crust are well illuminated by seismic ray coverage, therefore at least three to four times crossing between Lianxian and Gangkuo (Figure 4), and allow us to conclude that our model of crustal velocity and Moho depth for the most part of the profile is well-constrained (the northwest segment of the middle-lower crustal model limited by the low S/N ratio on the shot gather of LX). The Moho depths from our interpretation are consistent with those determined from gravity inversion (Zeng *et al.*, 1997) and other wide-angle seismic profiles in the South China continent (Yuan *et al.*, 1989; Zhang *et al.*, 2000, 2005).

The Bouguer gravity anomaly along the Lianxian-Gankou profile varies between -5 mGal in the northwest and -1 mGal in the southeast (Yan et al., 2005). We construct an initial density model by converting the *P*-wave velocities into densities using the linear velocity-density relationship $\rho = a + bV_P$, where a = 0.0546 g/cm3, b = 0.3601 g.s/km.cm^3

(Christensen and Mooney, 1995). Then, we derive the crustal density distribution model (lower panel of Figure 3c) iteratively until we obtain a suitable fitting between the observed and calculated gravity anomaly. In our calculation, the mismatch between the calculated gravity anomaly from our final model and the observed gravity anomaly is less than 0.1 mGal (upper panel of Figure 3c). The uppermost crustal layer under the Lianxiang-Gankou profile is largely modelled with a density of 2.60-2.7 g/cm^3 and a low value of 2.45-2.65 g/cm^3 at Huiyuan Basin (Figure 3c). The middle crust exhibits densities of about 2.75 g/cm^3. The embedded low-velocity layer over the lower crust has a density of about 2.7 g/cm^3. Lastly, the lower crust has a density of about 2.9 g/cm^3.

The variation of crustal velocity structure corresponds to the gradual decrease of gravity anomaly from southeast to northwest in the gravity anomaly map of this studied area (Zeng et al., 1997; Yan et al., 2004), which can be seen the Bouguer gravity anomaly variation along the profile shown in the upper panel of Figure 3c. The negative gravity anomalies of limited spatial extent are interpreted as caused by the extensively distributed granites in South China block (Zeng *et al.*, 1997; Yan et al., 2004). As gravity anomaly field in South China is characterized with intense anomalies, the additional density deficiency may be produced by the granitization of crust (Matin *et al.*, 1994; Zeng *et al.*, 1997; Zhou and Li, 2000; Wang *et al.,* 2003). However, with limited spatial resolution of this wide-angle seismic experiment here, we cannot provide such evidences.

4. Crustal boundary between Yangtze and Cathaysia blocks

The final model of the *P*-wave crustal structure, infers that the Wuchuan-Sihui fault is a crust-scale feature that defines the boundary between the Yangtze and Cathaysia blocks. This fault extends from the surface of the W-S fault to the Moho, imaged by a series of *Pn* refracted events from Moho (Poppeliers and Levander, 2004). The lower crust and uppermost mantle beneath the segment 140-240 km along the profile (Figures 2b and 2d) shows a mantle topography that produces the irregular scattering from the Moho interface or a stochastic structure featured with multiple *Pn* refractions, not laterally consistent intra-crustal *P3*, *P4* reflections and strong *Pm* seismic reflection responses (Poppeliers and

Levander, 2004), which may indicate strong crust-upper mantle interaction. The changes in the velocity model define the crustal boundary between the Yangtze and Cathaysia blocks.

From the velocity model (Figure 3b) and density model (Figure 3c), we may infer the Wuchuan-Sihui fault as the boundary between the Yangtze and the Cathaysia blocks. Geochemical evidence also supports our interpretation of the feature of the boundary between the Yangtze and the Cathaysia blocks (Wang *et al.*, 2003). Mafic rocks west of the Chenzhou-Linwu fault (the northward extension of Wuchuan-Sihui fault, Figure 1) commonly show an EMI-like isotopic affinity marked by relatively low Sr87/Sr86 ratio, LREE enrichment and high LILE/HFSE ratios. In contrast, mafic rocks to the east of the fault show a prevalent EMII-like isotopic signature, with significantly higher Sr87/Sr86 and relatively low LILE/HFSE ratios (Wang *et al.,* 2003). This indicates that Mesozoic mafic rocks around the Chenzhou-Linwu-Wuchuan-Sihui fault have a distinct affinity to enriched lithospheric mantle and tectonic histories. The spatial variation of EMI-EMII-like signatures within Mesozoic mafic rocks around the Chenzhou-Linwu-Wuchuan-Sihui fault; the westward verging Early Mesozoic fold and thrust belt and important multi-metal mineralization may shed some light on the nature of the lithospheric boundary between the Yangtze and Cathaysia blocks (Gilder *et al.*, 1996; Wang *et al.,* 2003)

.

5. Continent-ocean transition section

We construct a cross-section covering the continent-ocean transition between the continental South China and the South China Sea in order to understand the lateral variation across the continental margin of South China Sea. As shown in Figure 5, in addition to this Lianxian-Gangkou profile, there are two more wide-angle seismic profiles (Tunxi-Wenzhou profile and Hengyang-Quanzhou profile) conducted in 1990s across the south China continent, and three ocean-bottom seismometer (OBS) geophysical experiments (ESP-W, ESP-C and ESP-E) carried out across the northern margin of the South China Sea (Yuan *et al.*, 1989; Nissen *et al.*, 1995a,b; Yan *et al.*, 2001; Zhang *et al.,* 2005). Based on these six profiles, we construct a cross-section AA' in excess of 1000 km

length, from the Yangtze block to the South China Sea, by projecting the Moho depths of these six profiles onto the NW-SE profile.

The cross-section (Figure 6) shows that crustal thickness ranges within 34-36 km in Yangtze block, 30-32 km in the Cathaysia block, and 26-28 km in the north continental margin of South China Sea, with a remarkable thinning to 8-15 km under the South China Sea, or 10-12 km under the South China Sea from satellite-derived gravity field (Braitenberg *et al*., 2006). We can see a 2-3 km abrupt thinning of crustal thickness from the Yangtze block to the Cathaysia block, at least 4 km thinning of crustal thickness at the about 100 km-long continent-sea transition zone in the south China continental margin, and at least 10 km thinning of crustal thickness from the margin of the South China Sea to the South China Sea. Figure 6 demonstrates that the Moho depth shallows smoothly from the Yangtze block to the Cathaysia, and to the north margin of South China Sea, and then shallows abruptly to the South China Sea.

6. Conclusions

The NW-SE wide-angle seismic profile from Lianxian to Gangkou has lead to a quantitative model of the crust-upper mantle *P*-wave velocity structure in the South China. A thick sedimentary layer covering the whole profile has an average thickness of about 4 km (except about 6 km under Minzhong Depression near to Qinyuan and Huiyuan Basin near to Boluo) and the *P*-wave velocity V_P < 6.0 km/s. The velocity structure model distinguishes upper, middle and lower crustal layers. The upper crust has strong lateral variation in the *P*-wave velocity. The comparatively thin middle crust consists of two layers, the lower layer, a narrow, low-velocity channel that has very little lateral variation in velocity.

The seismic profile identifies the evidences of major crustal penetrating active faults. In particular, the Wuchuan-Sihui fault is the crustal boundary between the Yangtze and the Cathaysia blocks.

Combining this seismic profile with other five profiles, we construct a cross-section of 1000 km length, from the Yangtze block in the continental to the South China Sea. This

continent-ocean transition profile shows that the Moho depth shallows gradually from the Yangtze block to the Cathaysia block and the north margin of South China Sea, and then shallows abruptly to the South China Sea.

Acknowledgements

This project was supported by National Nature Science Foundation of China (40304007, 40474034, 49825108 and 40230056) and Chinese Academy of Sciences (KXCX2-109). We are indebted to Prof. Zhouxun Yin, Drs. Tao Xu, Xi Zhang, Zhiming Bai, Bin Zhao and others who gracefully supplied us geophysical information and who did the seismic data acquisition of the CAS Institute of Geophysics, and to Professors Jiwen Teng, Xiangru Kong and Yafeng Yan for their constructive comments and suggestions. Prof. George Helffrich and two anonymous reviewers have provided critical reviewing that improves the clarity of this presentation.

References

Angelier, J., 1990. Inversion of field data in fault tectonics to obtain the regional stress –III: A new rapid direct inversion method by analytical means. Geophys. J. Int. 103, 363-376.

Avendonk, H., 2004. Slowness-weighted diffraction stack for migrating wide-angle seismic data in laterally varying media. Geophysics 69, 1046–1052.

Braitenberg, C., Wienecke, S. and Wang, Y., 2006. Basement structures from satellite-derived gravity field: South China Sea ridge. J. Geophys. Res., 111, B05407, doi: 10.1029/2005JB003938.

Červený, V., Molotkov, I.A., Pšenčík, I., 1977. Ray methods in seismology. University of Karlova, Prague.

Charvet, J., Shu, L.S., Shi, Y.S., Guo, L.Z., Faure, M., 1996. The building of south China: Collision of Yangzi and Cathaysia blocks, problems and tentative answers. J. Southeast Asian Earth Sci. 13, 223-235.

Chen, J.F., Jahn, B.M., 1998. Crustal evolution of south-eastern China: Nd and Sr isotopic

evidence. Tectonophysics 284, 101-133.

Christensen, N. I., and W. D. Mooney, 1995. Seismic velocity structure and composition of the continental crust: A global view, J. Geophys. Res., 100, 9761-9788.

Cook F. A., 2002. Fine structure of the continental reflection Moho. Geol. Soc. Am. Bulletin 114, 64-79; DOI: 10.1130/0016-7606.

Faure, M., 1996. Extensional tectonics within a subduction-type orogen: the case study of the Wugongshan dome (Jiangxi Province, south-eastern China). Tectonophysics 263, 77-106.

Funck, T., Louden, K.L., Hall, J., 2001, Wide-angle reflectivity across the Torngat Orogen, NE Canada. Geophys. Res. Lett. 28, 3541-3544.

GBGMR (Guangdong Bureau of Geology and Mineral Resources), 1989. Regional geology survey in Guangdong Province: Beijing, China, Geological Press (in Chinese).

Gilder, S.A., Gill, J., Coe, R.S., 1996. Isotopic and Paleo-magnetic constraints on the Mesozoic tectonic evolution of south China. J. Geophys Res. 107(B7), 16137-16154.

Grabau, A.W., 1924. Migration of geosynclines. Geol. Soc. China Bull. 3, 207–349.

Guo, L.Z., Shi, Y.S., Ma, R.S., 1983. On the formation and evolution of the Mesozoic–Cenozoic active continental margin and island arc tectonics of the western Pacific Ocean. Acta Geol. Sin. 1, 11–21.

Holloway, N., 1982. North Palawan block, Philippines: its relation to the Asian mainland and role in evolution of South China Sea. Am. Asso. Petrol. Geol. Bull. 66, 1355-1383.

Hou, Q.L., Li, J.L., 1993. A preliminary study on the foreland fold and thrust belt, southwest Fujian. In: Li, J.L. (Ed.), Lithospheric Structure and Geological Evolution of Southeastern Continent. Metallurgical Publishing House, Beijing, 264 pp.

Hsü, K.J., Sun, S., Li, J.L., Chen, H.H., Pen, H.P., Sengör, A.M.C., 1988. Mesozoic overthrust tectonics in south China. Geology 16, 418–421.

Hsü, K.J., Li, J.L., Chen, H.H., Wang, Q.C., Sun, S., Sengör, A.M.C., 1990. Tectonics of South China: key to understanding west Pacific geology. Tectonophysics 183, 9–39.

Huang, T.K. (Ed.), 1980. Tectonic Evolution of China: Explanatory Notes for 1: 4,000,000 Tectonic Map of China. Sci. Publ. House, Beijing, 124 pp.

Jahn, B.M., Martineau, F., Peucat, J.J., Cornichet, J., 1986. Geochronology of the Tananao

Schist complex, Taiwan. Tectonophysics 125, 103–124.

Jahn, B.M., Zhou, X.H., Li, J.L., 1990. Formation and tectonic evolution of Southeastern China and Taiwan: isotopic and geochemical constraints. Tectonophysics 183, 145–160.

Li, J.L., Sun, S., Hsü,, K.J., Chen, H.H., Peng, H.P., Wang, Q.C., 1989. New evidence about the evolution of the South Cathaysia Orogenic Belt. Sci. Geol. Sin. 3, 217–225.

Li, J.L. (ed.), 1992. Study on the Texture and Evolution of the Oceanic and Continental Lithosphere in Southeastern China. Chinese Science and Technology Press, Beijing.

Li, X., McCulloch, M., 1996. Secular variation in the Nd isotopic composition of Neoproterozoic sediments from the southern margin of the Yangtze block: evidence for a Proterozoic continental collision in southeast China. Precambrian Res. 76, 67-76.

Li, X., Sun, M., Wei, G.J., Liu, Y., Lee, C.Y., Malpas, J., 2000. Geochemical and Sm–Nd isotopic study of amphibolites in the Cathaysia Block, southeastern China: evidence for an extremely depleted mantle in the Paleoproterozoic. Precambrian Res. 102, 251-262.

Lin, G., Wang, Y.H., 2005. The P-wave velocity structure of the crust-mantle transition zone in the continent of China. J. Geophys. Eng. 2, 268-276.

Martin, H., Bonin, B., Capdevial, R., Jahn, B.M., Lameyre, J., Wang, Y., 1994. The Kuiqi peralkaline granitic complex (SE China): petrology and geochemistry. J. Petrol. 35, 983–1015.

Morozov, I.B., Levander, A., 2002. Depth image focusing in travel-time map based wide-angle migration. Geophysics 67, 1903 - 1912.

Németh B., Z. Hajnal and S. B. Lucas, 1996, Moho signature from wide-angle reflections: preliminary results of the 1993 Trans-Hudson Orogen refraction experiment. Tectonophysics 264, 111-121

Nissen, S., Hayes, D., Buhl, P., Diebold, J., Yao B., Zeng W., Chen Y., 1995a. Deep penetration seismic sounding across the north margin of South China Sea. J. Geophys. Res. 100(B11), 22407-22433.

Nissen, S., Hayes, D., Yao, B., Zeng, W., Chen, Y., Nu, X., 1995b. Gravity, heat flow, and

seismic constraints on the processes of crustal extension: Northern margin of South China Sea. J. Geophys. Res. 100(B11), 22447-22483.

Poppeliers, C., Levander A., 2004. Estimation of vertical stochastic scale parameters in the Earth's crystalline crust from seismic reflection data, Geophys. Res. Lett. 31.

Qiu, Y., Gao, S., McNaughton, N., Groves, D., Ling, W., 2000. First evidence of >3.2 Ga continental crust in the Yangtze craton of South China and its implications for Archean crustal evolution and Phanerozoic tectonics. Geology 28, 11-14.

Ren, J.S., Chen, T.Y., Niu, B.G., Liu, Z.G., Liu, F.R., 1990. Tectonic Evolution of the Continental Lithosphere and Metallogeny in Eastern China and Adjacent Areas. Science Press, Beijing, 205 pp.

Rodgers, J., 1989. Comments on Mesozoic overthrust tectonics in south China. Geology 17, 671–672.

Rowley, D.B., Ziegler, A.M., Nie, G., 1989. Comment on Mesozoic overthrust tectonics in south China. Geology 17, 394– 396.

Shui, T., 1988. Tectonic framework of the continental basement of southeast China. Sci. Sin., Ser. B 31, 885–896.

Wang, E.K., Liu, C., 1992. Is the Cathaysia a unified block? Geology of collisional orogenic belts in Early Mesozoic in Fujian and Guangdong. In: Li, J.L. (ed.), 1992. Study on the Texture and Evolution of the Oceanic and Continental Lithosphere in Southeastern China. Chinese Science and Technology Press, Beijing, pp. 96-105.

Wang, Y.J., Fan, W., Guo, F., Peng, T., Li, C., 2003, Geochemistry of Mesozoic mafic rocks adjacent to the Chenzhou-Linwu fault, south China: implications for the lithospheric boundary between the Yangtze and Cathaysia blocks. Internat. Geol. Reviews, 45, 263-286.

Wei, S., Teng, J., Wang, Q., Zhu, Z., 1990, Crust and mantle structure in the East China, China Science Press.

Xu, S.T., Sun, S., Li, J.L., Jiang, L.L., Chen, G.B., Shi, Y.H., 1993. Lantian structural window. Sci. Geol. Sin. 2, 105–116.

Yan, P., Zhou, D., Liu, Z., 2001. A crustal structure profile across the northern continental margin of South China Sea. Tectonophysics 338, 1-21.

Yan Y.F., Wang G.J., Zhang Z.J., 2004. Characteristics and tectonic significance of the gravity field in South China. Acta Geologica Sinica 78 (6): 1235-1244.

Yang, Z.Y., Chen, Y.Q., Wang, H.Z., 1986. The Geology of China. Clarendon, Oxford, 303 pp.

Yin, A., Nie, S.Y., 1993. An indentation model for the north and south China collision and the Tan-Lu and Honam fault systems, eastern Asia. Tectonics 4, 801–813.

Yuan, X.C., Zuo, Y., Cai, X.L., Zhu, J.S., 1989. The structure of the lithosphere and the geophysics in the South China Plate. In: Progress on Geophysics in China in the 1980s, edited by the editorial board of Bulletin of Geophysics, Beijing, pp. 243–249 (in Chinese and with English abstract).

Zeng, H., Zhang, Q., Li, Y., Liu, J., 1997. Crustal structure inferred from gravity anomalies in South China. Tectonophysics 283, 189-203.

Zhang, L.G., Wang, K.F., Chen, Z.S., Liu, J.X., Yu, G.X., Wu, K.L., Lan, J.Y., 1994. On Cathaysia: evidence from lead isotope study. Geol. Rev. 3, 200–208.

Zhang, Z.J., Wang, G., Teng, J., Klemperer, S., 2000, CDP mapping to obtain the fine structure of crust and upper mantle: An example in the Southeastern China. Phys. Earth Planet. Interiors 122, 131-144.

Zhang, Z.J., Badal, J., Li, Y., Chen, Y., Yang, L., Teng, J., 2005, Crust-upper mantle seismic velocity structure across Southeastern China. Tectonophysics 395, 137-157.

Zhang, Z.M., Liou, J.G., Coleman R.G., 1984. An outline of the plate tectonics of China. Geol. Soc. Am. Bull. 95, 295-312.

Zhou, X., Li, W., 2000. Origin of Late Mesozoic igneous rocks in Southeastern China: implications for lithospheric subduction and underplating of mafic magmas. Tectonophysics 326, 269-287.

Figure Captions

Figure 1. Location map of the Lianxian-Gangkou wide-angle seismic experiment. Triangles and stars mark the geographical positions of stations and shot points, respectively. The major active faults crossed by the seismic profile from the northwest to the southeast are: F_1, Wuchuan-Sihui fault, F_2, Enping-Xinfeng fault, F_3, Heyuan-Zengcheng fault, F_4, Zijjin-Boluo fault and F_5, the Lianhuashan fault.

Figure 2. Upper panels: shot gathers (P-wave vertical-component) fired at six sites: (a) Lianxian (LX), (b) Dawan (DW), (c) Qingyuan (QY), (d) Conghua (CH), (e) Boluo (BL) and (f) Gankou Island (GK). Sections are reduced using a P-wave reduction velocity of 6.0km/s. The solid lines are the computed traveltimes for the crustal model. Lower panels: corresponding raypaths.

Fig. 3. (a) The velocity model of the upper crust from Pg and P_1 traveltime interpretation. Isolines of seismic velocity, given in km/s, emphasize different structures. The positions of the major active faults are shown on the surface where they intersect the profile. (b) The velocity model including the upper crust, middle crust, lower crust, Moho discontinuity and uppermost mantle. (c) Comparison between the observed (Zeng et al., 1997; Yan et al., 2005) and the calculated Burger gravity anomaly with the crustal density model converted from the crustal velocity model.

Fig. 4. Zones of the probed crust illuminated by ray coverage. Numbers 1 to 6 indicate the times that a seismic rays cross a portion of crust.

Fig. 5. Map of South China Tectonics. Spatial distribution of the wide-angle seismic profiles: Lianxian-Gangkou (this study), Hengyang-Quanzhou (Yuan *et al.*, 1989) and Tunxi-Wenzhou (Zhang *et al.*, 2005) and three OBS profiles in South China Sea (Nissen *et al.*, 1995a,b; Yan *et al.*, 2001). Here A-A' is the approximate location of the composite cross-section across the Yangtze block, Cathaysia block, and the north continental margin of South China Sea.

Fig. 6. Cross-section A-A' across South China. Shaded band shows the range of Moho depths from three wide-angle profiles and three OBS seismic experiments. Crustal thickness decreases from the northwest to the southeast as emphasized by the shaded band.

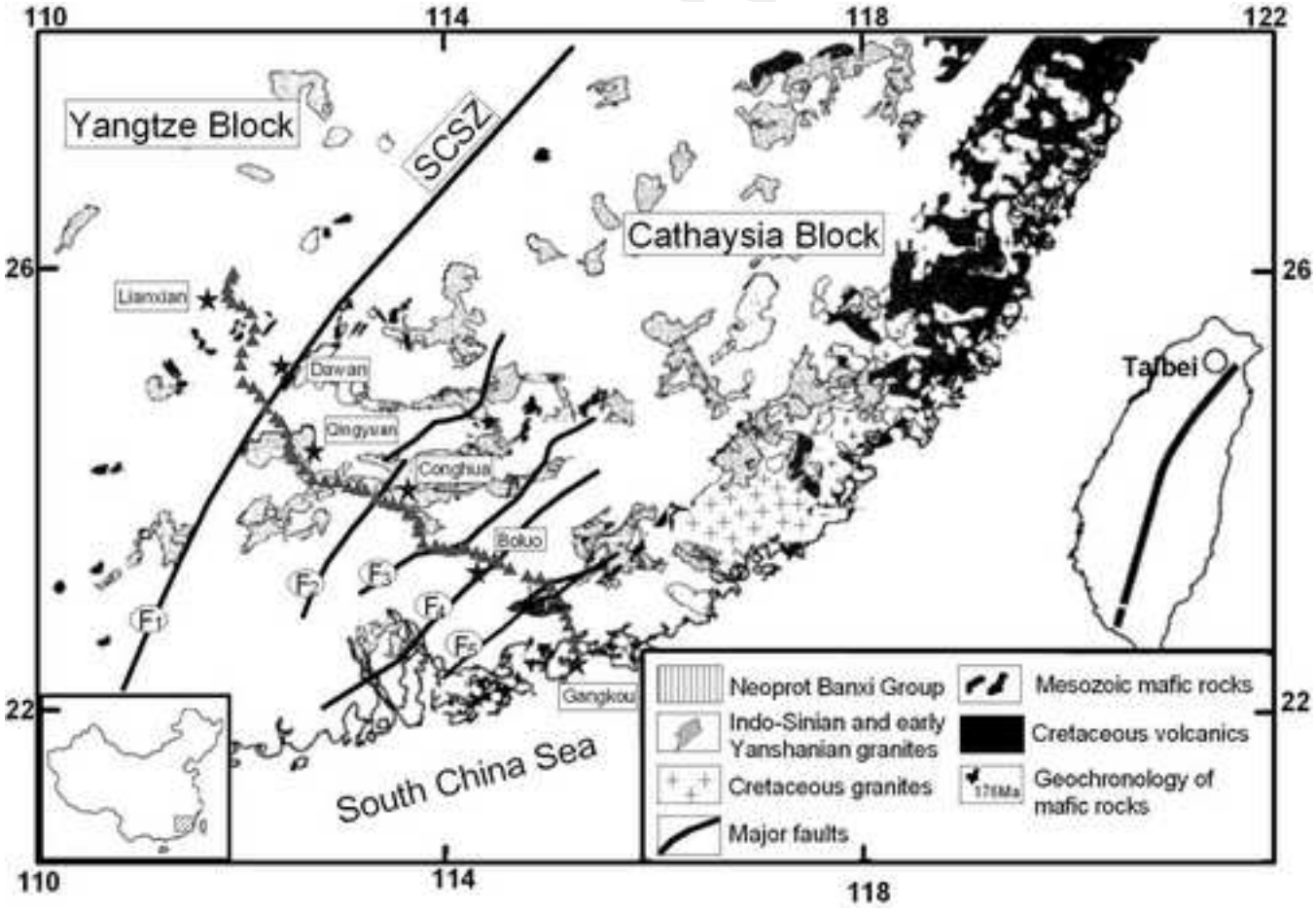

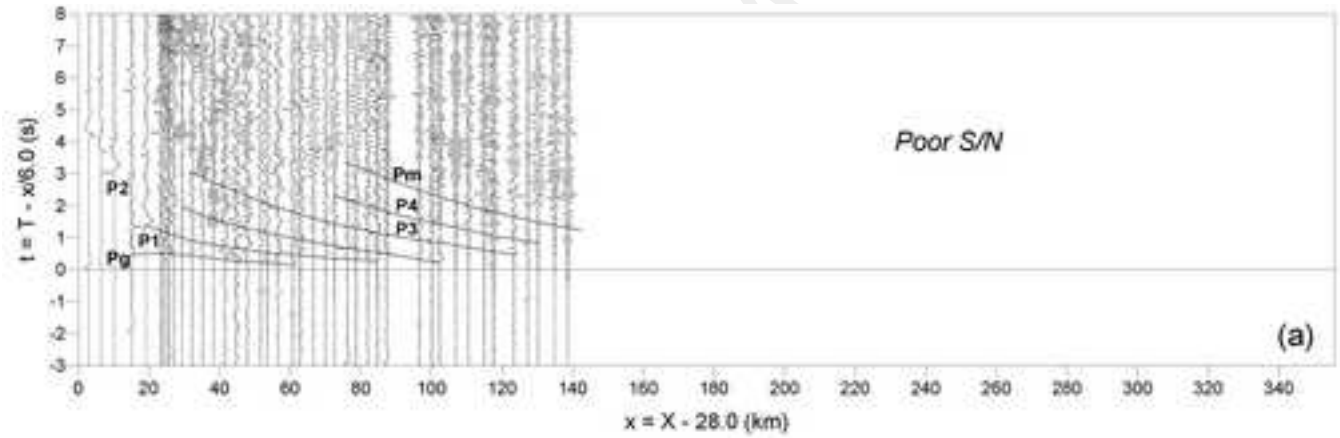

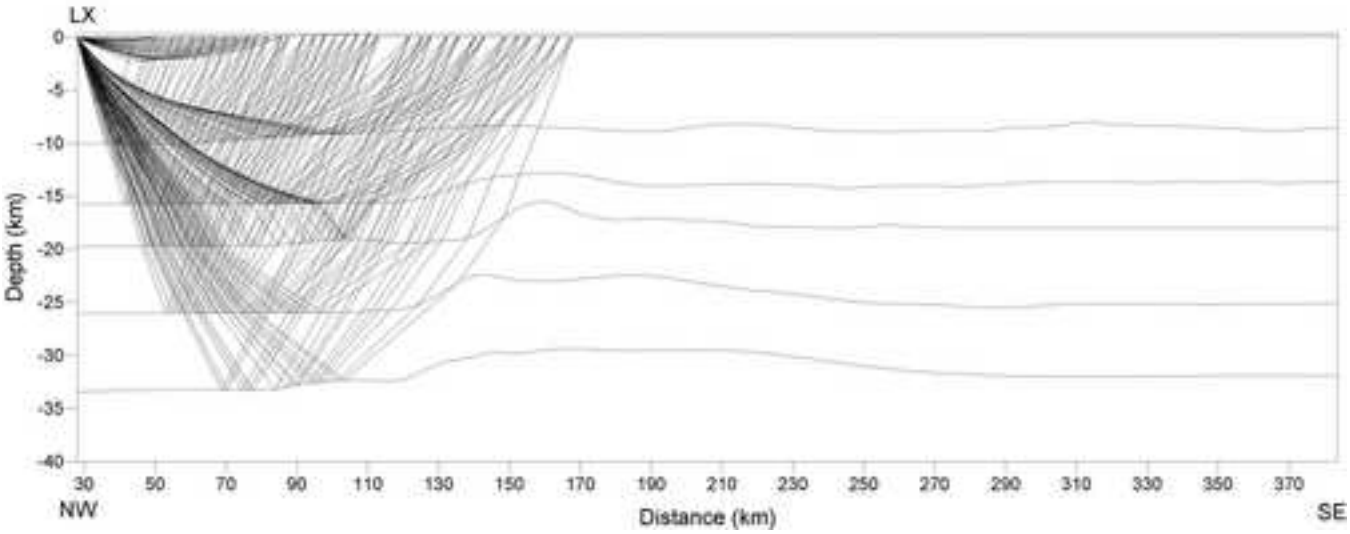

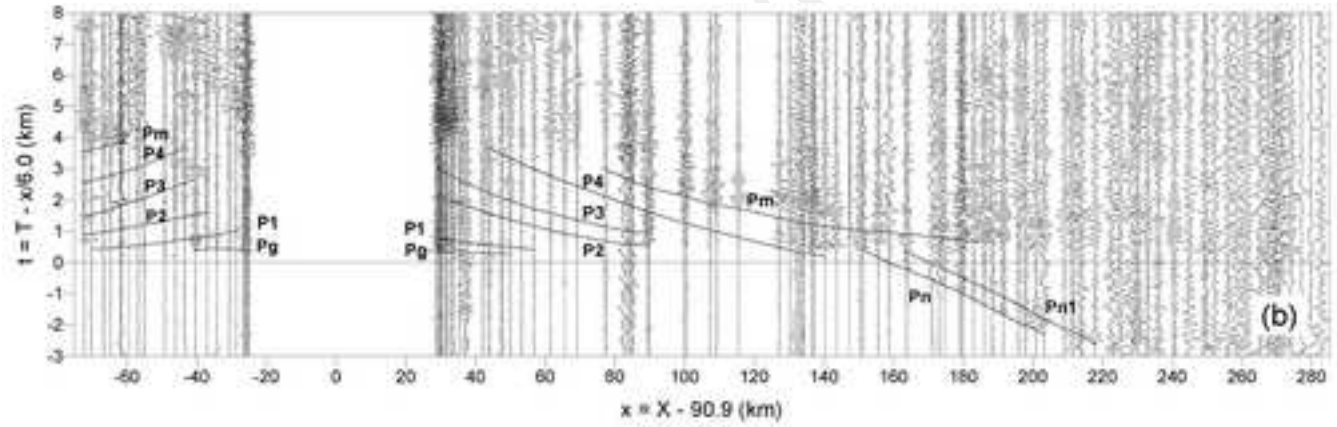

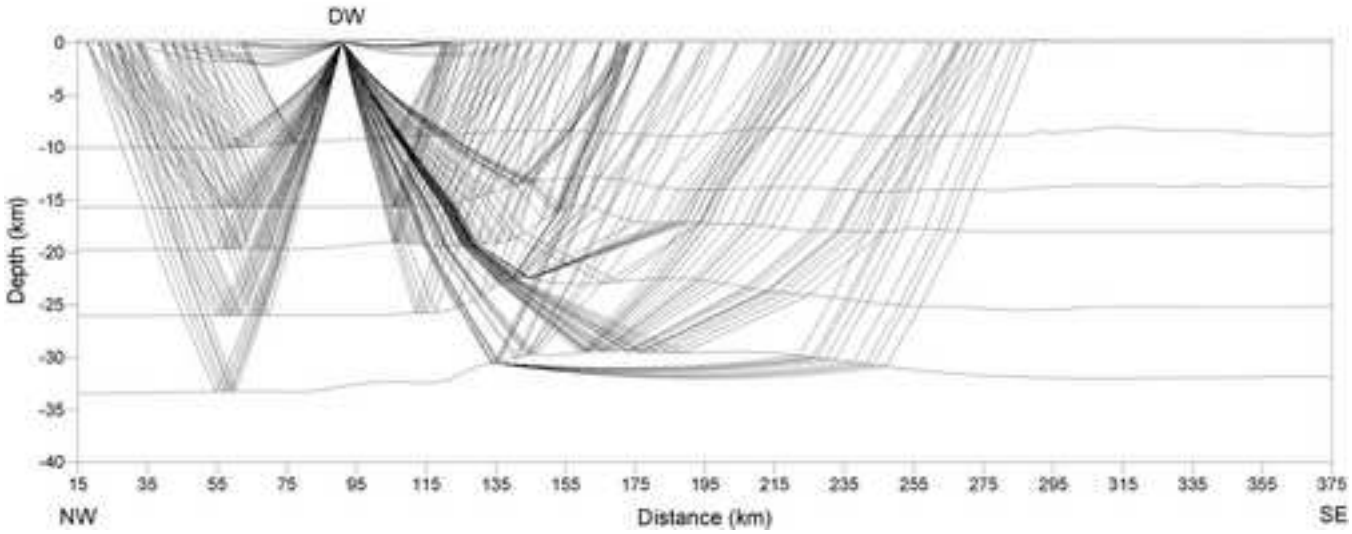

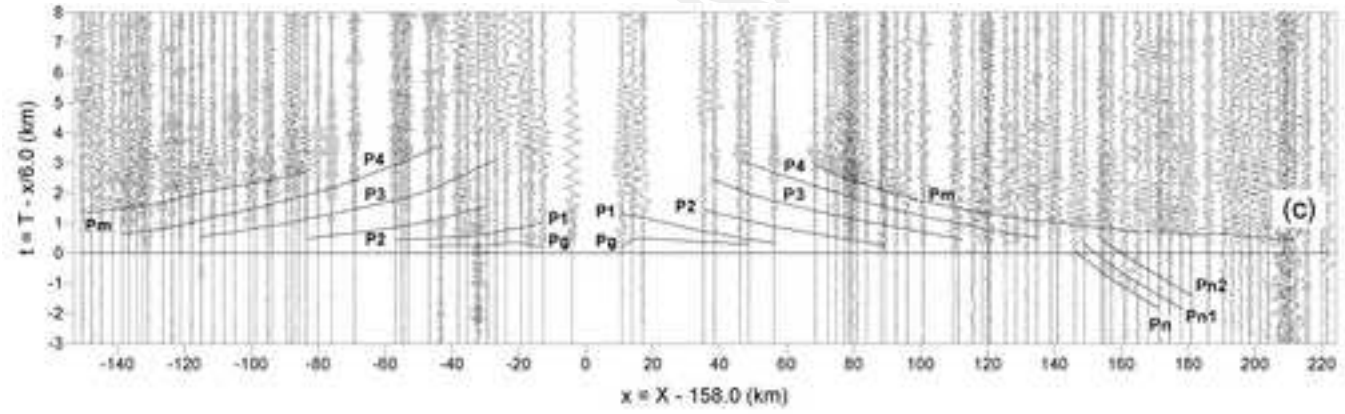

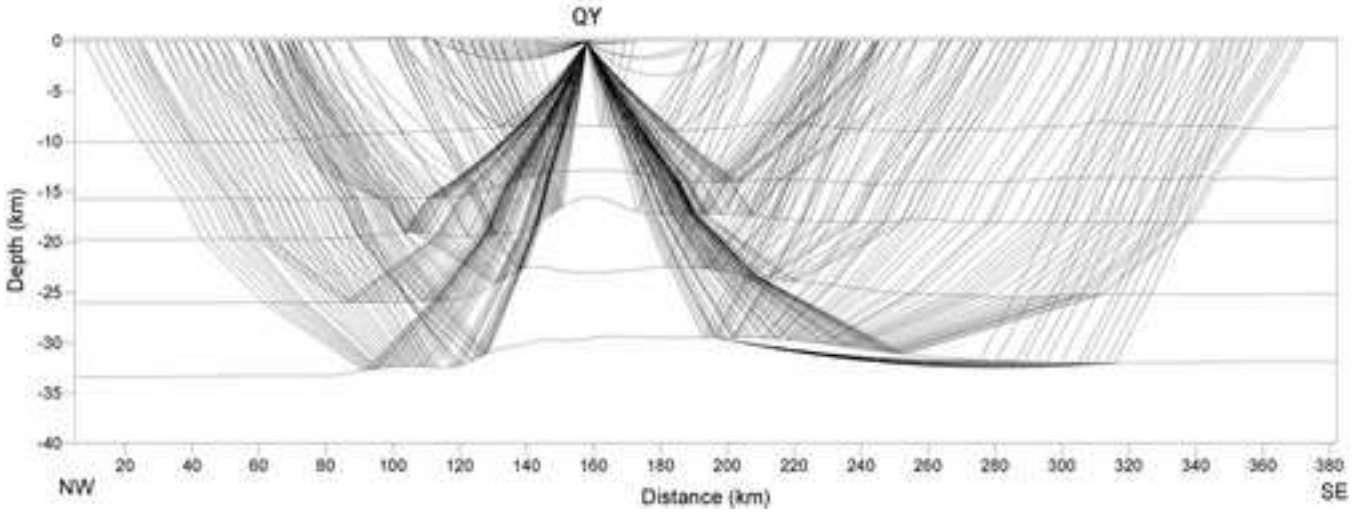

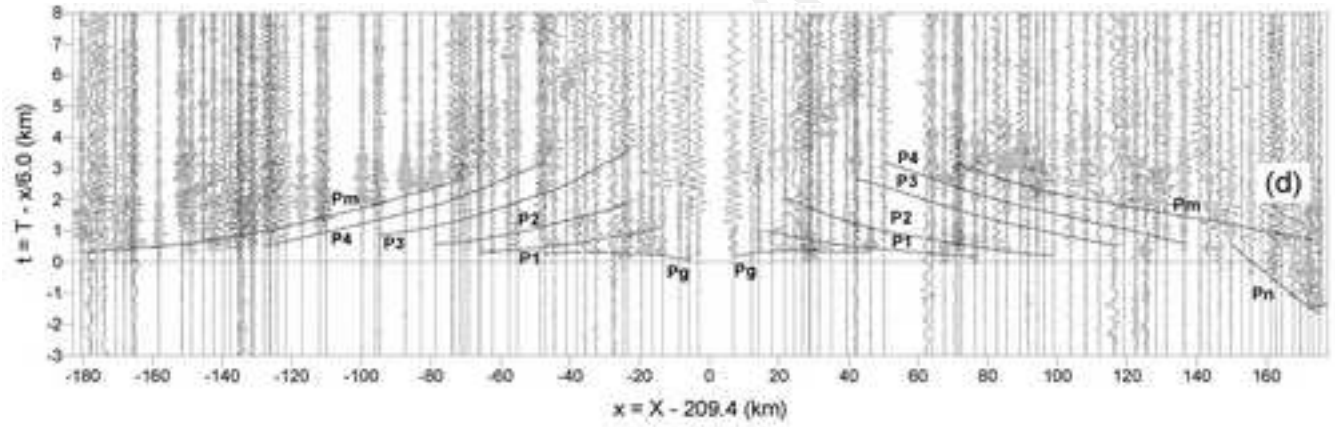

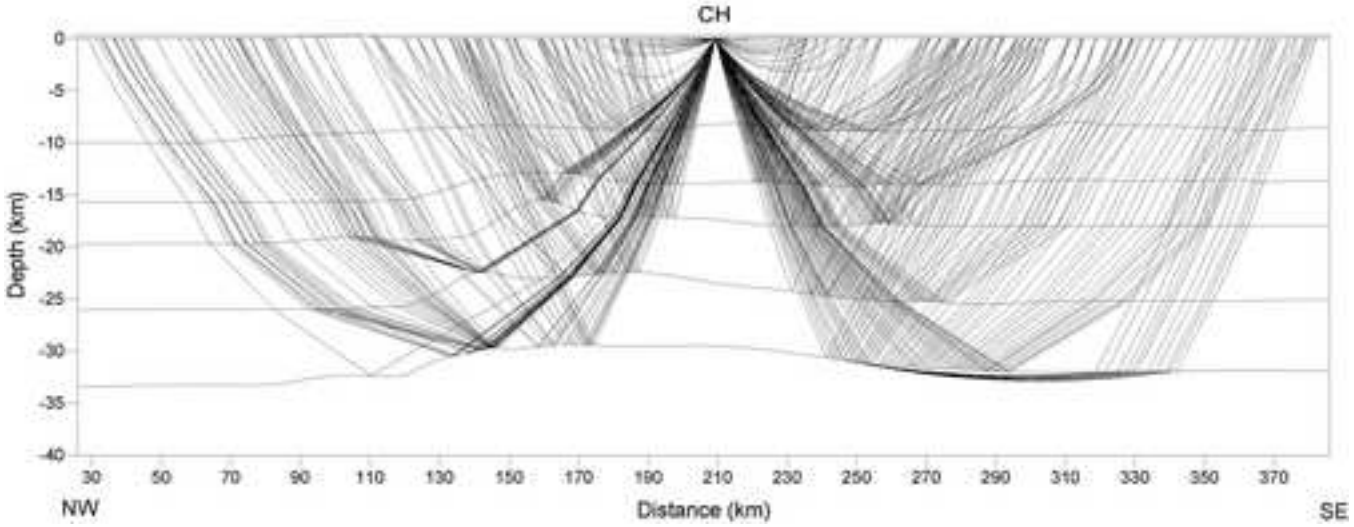

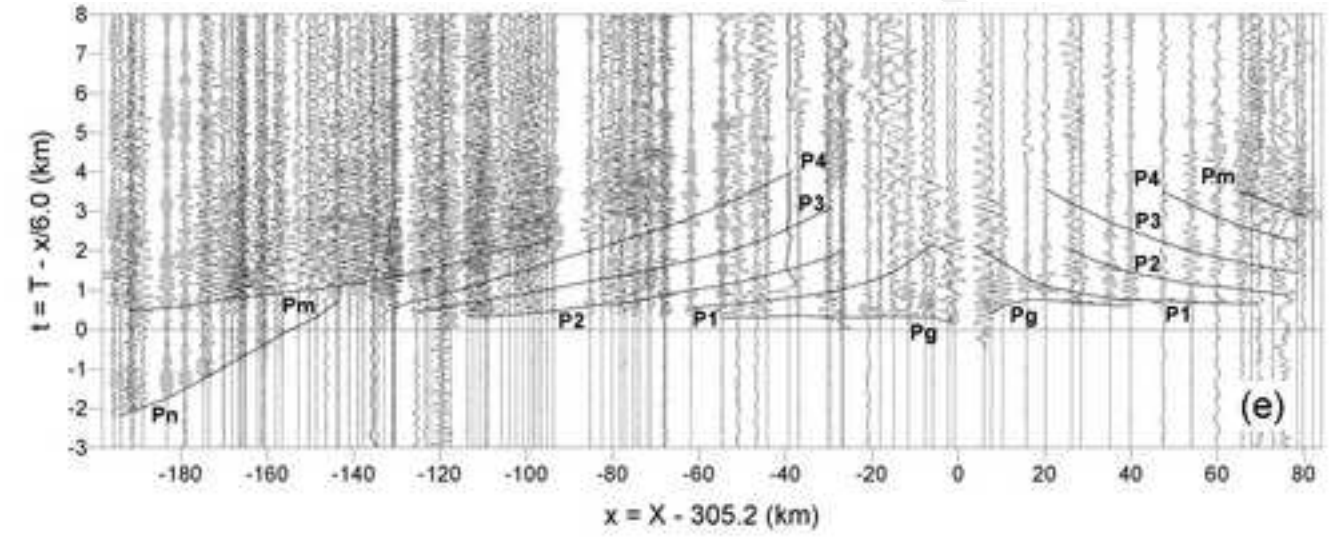

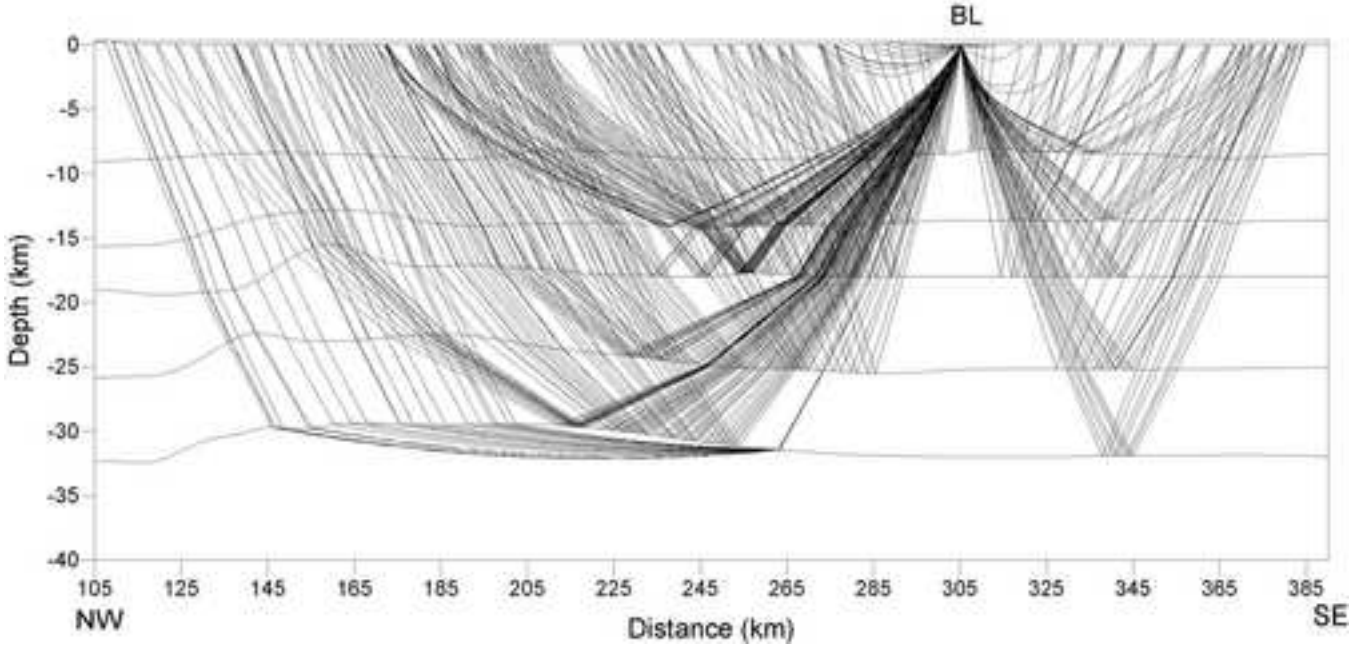

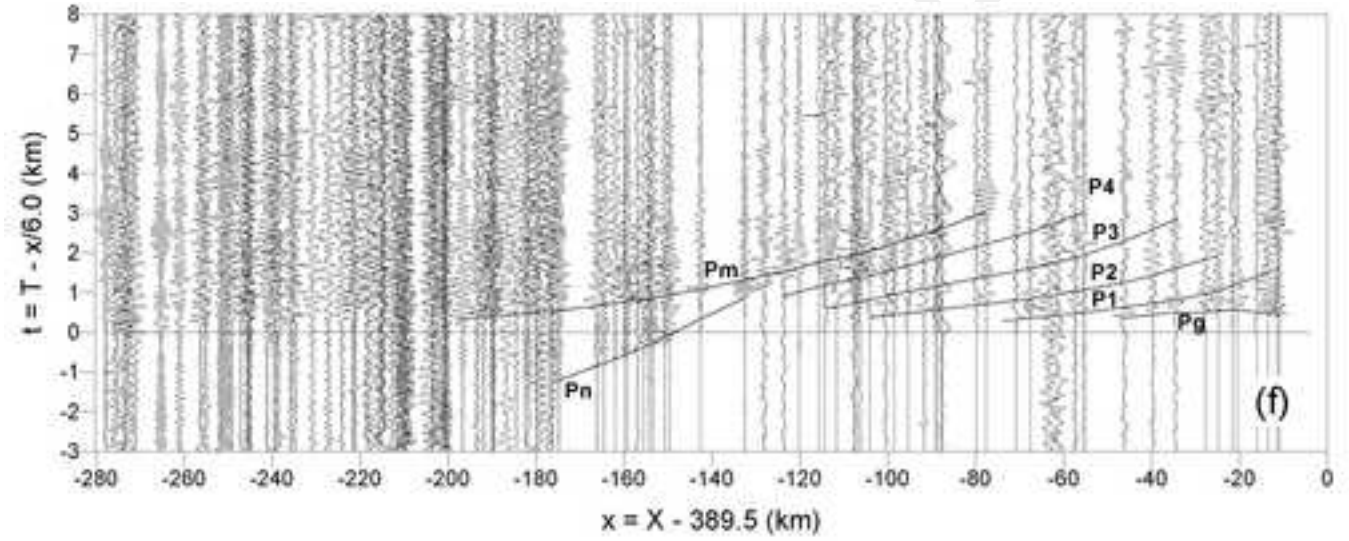

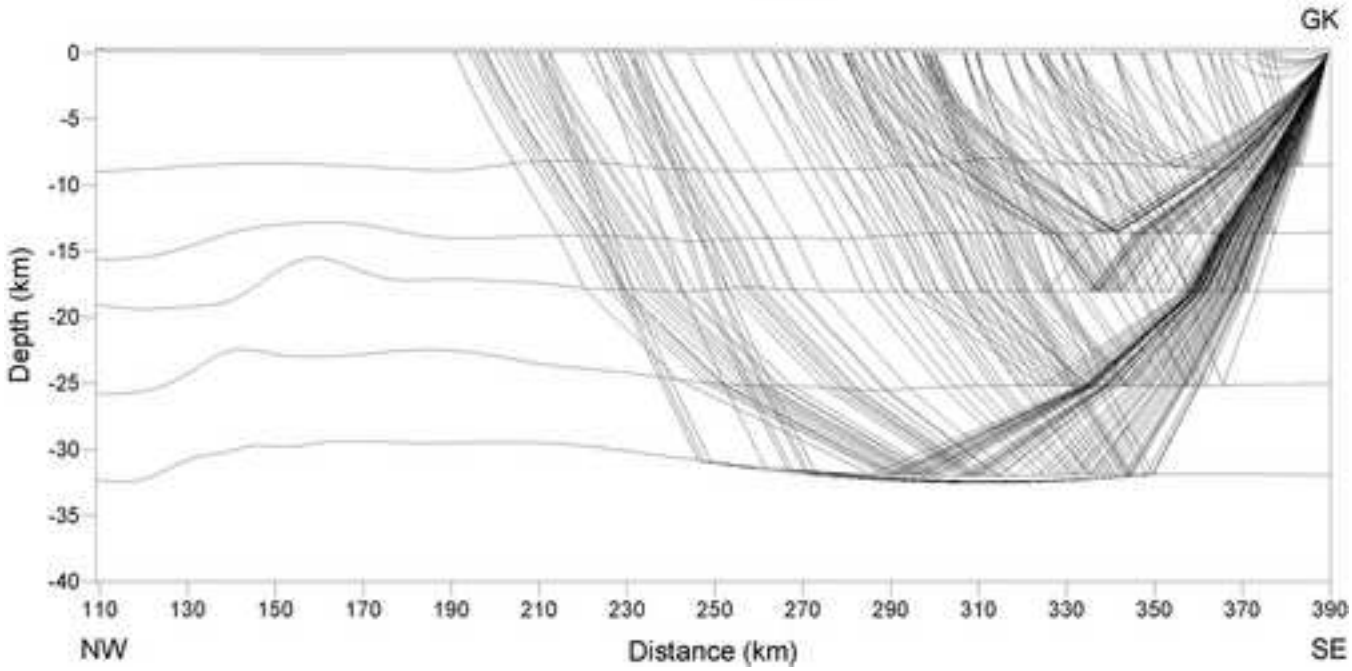

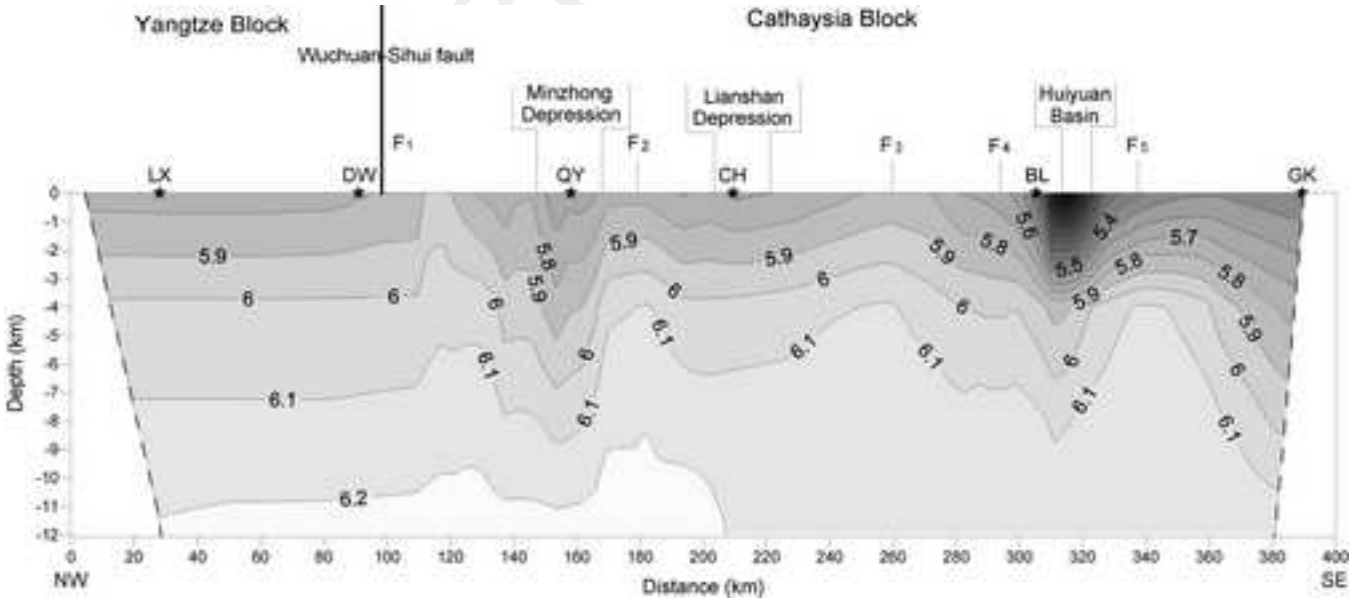

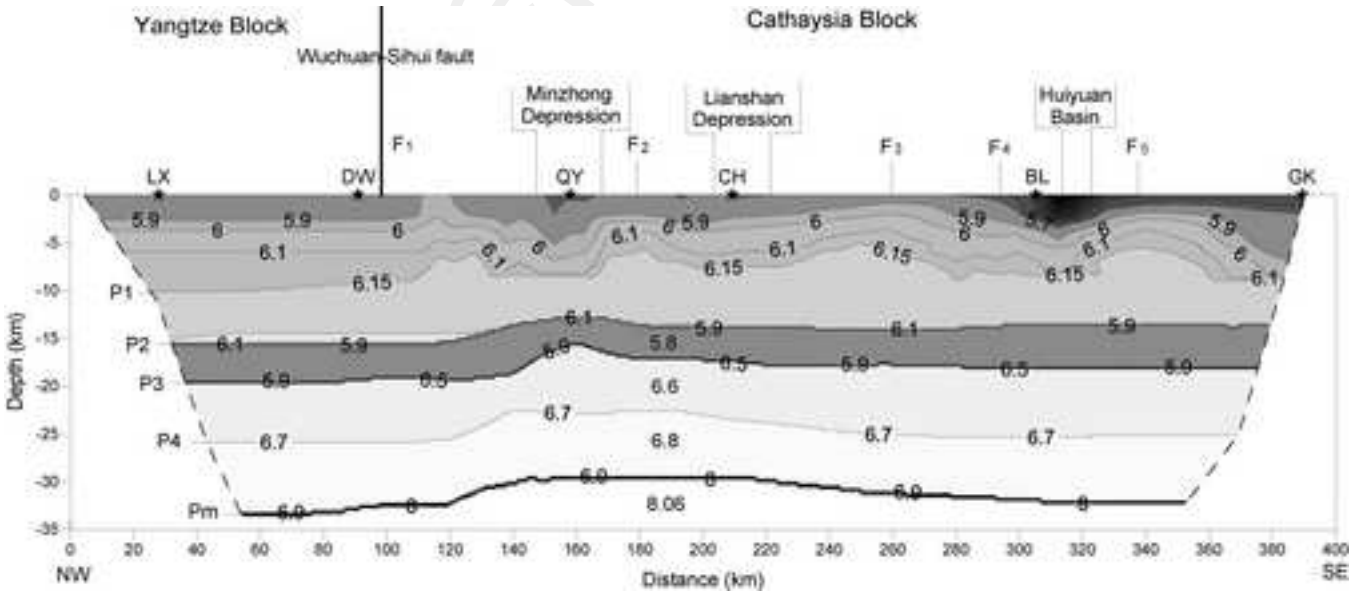

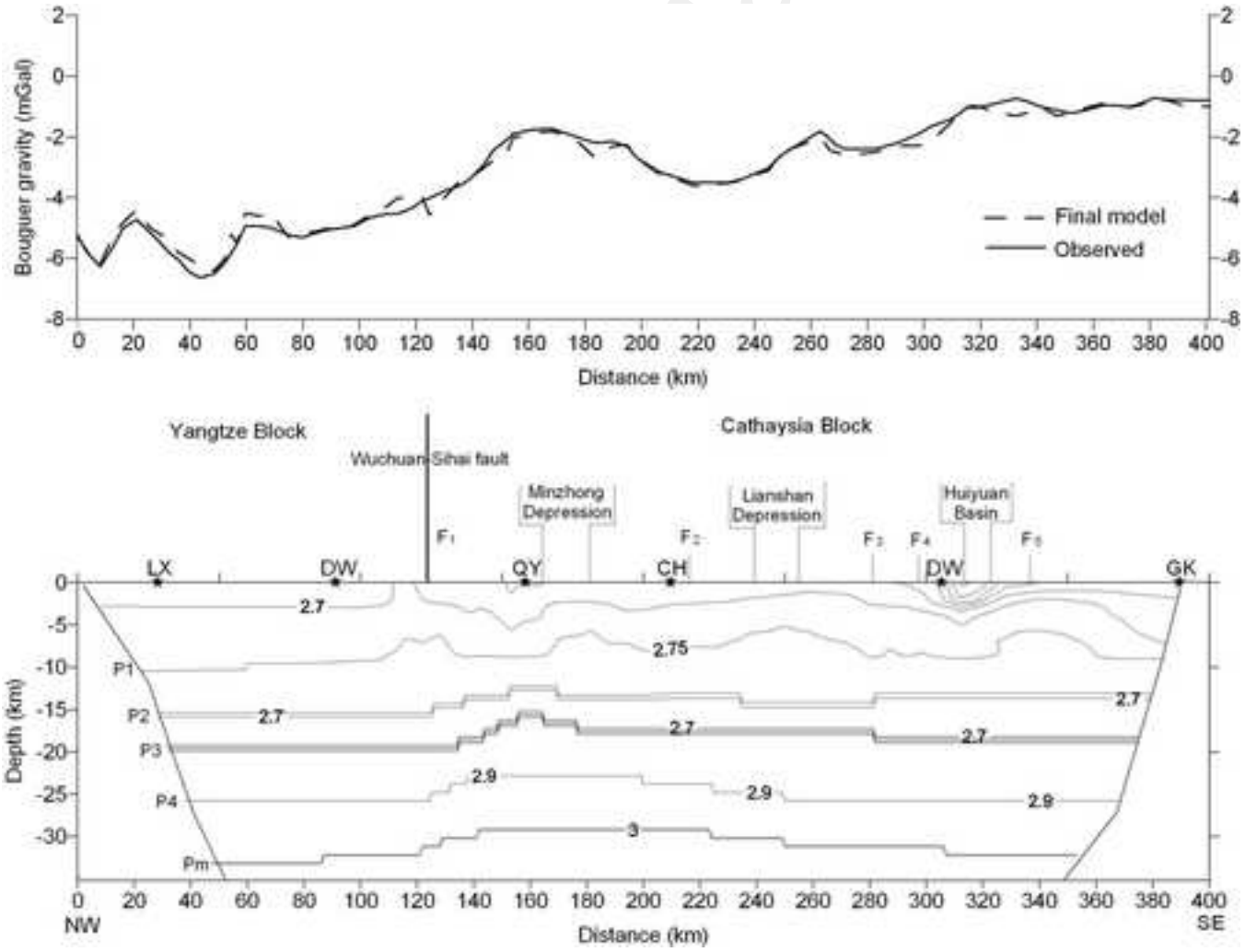

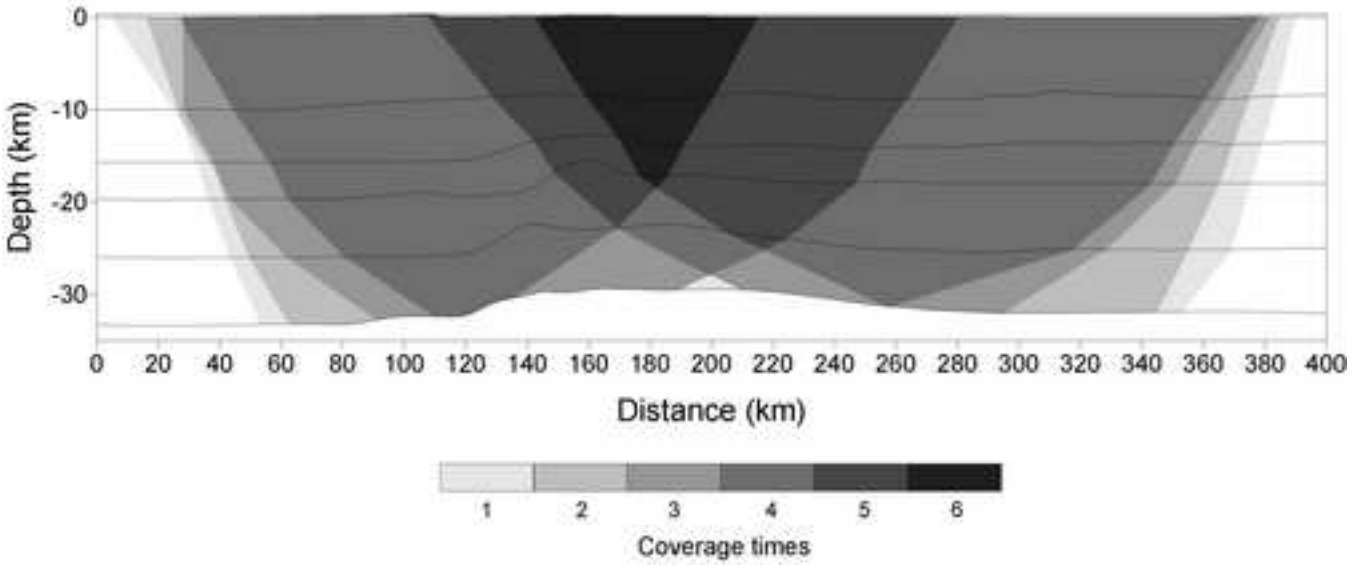

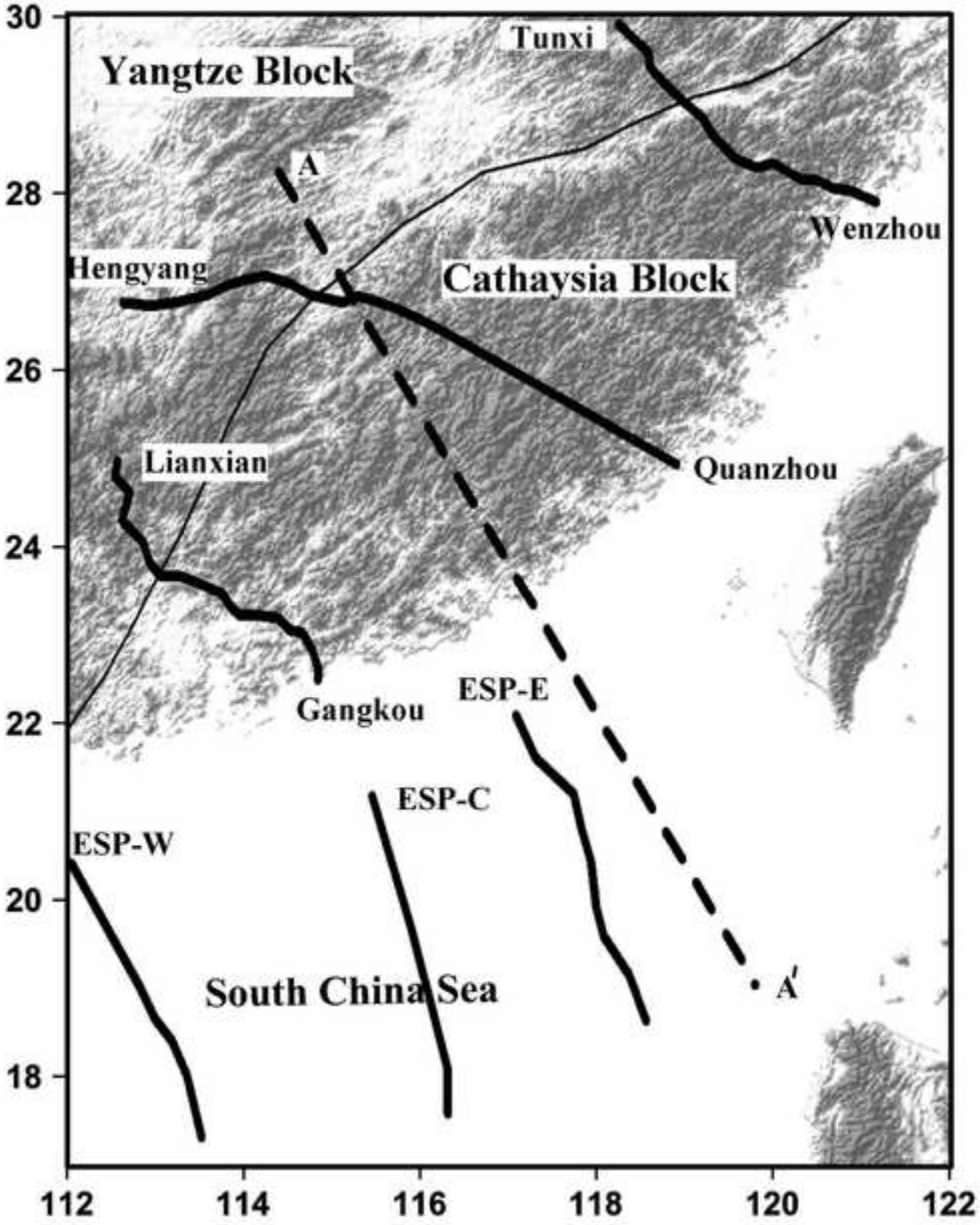

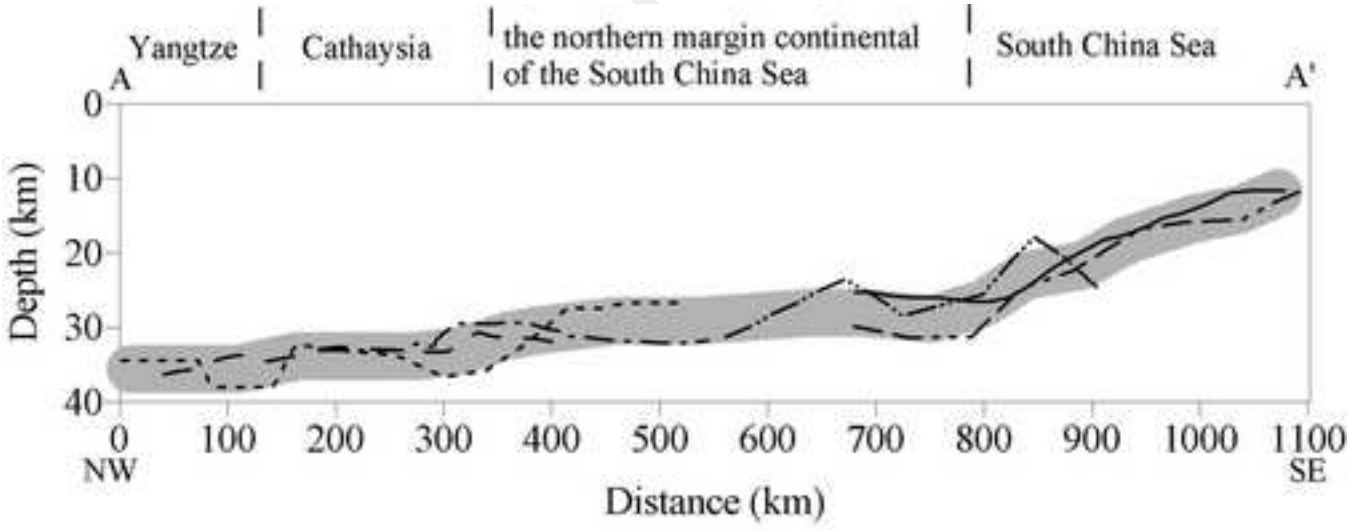

Vertical exaggeration 7:1

— — Tunxi - Wenzhou (Zhang et al., 2005)

------- Hengyang - Quanzhou (Yuan et al., 1989)

-·-·-·- Lianxian - Gangkou (Zhang and Wang, this study)

-·-·-·- ESP - W (Nissen et al., 1995a)

-·-·-·- ESP - E (Nissen et al., 1995a)

——— ESP - C (Yan et al., 2001)